Proc. of JSCE,
No. 191, July 1971

OUT-OF-PLANE BUCKLING OF SOLID RIB ARCHES BRACED WITH TRANSVERSE BARS

Tatsuro SAKIMOTO and Yoshio NAMITA***

SYNOPSIS

The out-of-plane buckling of a circular arch is studied. The arch is composed of two main ribs braced with transverse bars and is subjected to uniformly distributed radial forces (see Fig. 1). The analysis is carried out by means of transfer matrix method and both the field matrix of arched rod and point matrix are presented. Attention is given to the influences of the flexural rigidity, the number and the location of bracing bars on the buckling strength of arches. Buckling coefficients for various types of arch are calculated by trial and error method. Useful suggestions about the bracing method are obtained from the results of computations. The theoretical analysis is followed by model tests in order to verify the results of computation.

1. INTRODUCTION

The out-of-plane buckling of arches means, in this paper, an elastic buckling which occurs with both lateral flexure and torsion simultaneously under mainly axial thrust. As is well known, the lateral-torsional buckling is one of dominant instability problems of slender arch bridges. In order to design a slender arch bridge as an economical and safe structure, it is necessary to give it enough lateral stability. In ordinary arch bridges of parallel double arches, the two arched ribs are usually braced either with a truss or with transverse bars in order to give them a sufficient lateral rigidity. These bracings will be more effective for the double arches which are not stable when considered separately.

L. Östlund[3] and G. Wästlund[4] investigated lateral stability of bridge arches braced with transverse bars in comparison with the lateral buckling of straight bars braced with battens. Various factors about the transverse bars are discussed and many important qualities are reported. The equation for the deformation of the arch, hewever, is not described with enough strictness.

S. Kuranishi[2] studied the lateral-torsional buckling of two-hinge circular arch bridges, composed of two main arched girders, cross beams and lateral bracing, loaded by uniformly distributed vertical forces. Buckling coefficients of arches with flexible cross bars are computed by means of strain energy method. Besides, a reduction factor for torsional rigidity of the main arched girder due to the flexibility of transverse bars are obtained, but effects due to discontinuity of cross bars are not considered.

One of the authors[1] presented a fundamental equation for deformation of a curved rod and employed it to an analysis of out-of-plane buckling of single arch. In this paper, employing transfer matrix method to this fundamental equation, the authors describe the out-of-plane buckling of double arches braced with transverse bars. By means of this method, the buckling problem of double arches braced with arbitrary number of transverse bars in arbitrary location can be analyzed.

2. THEORETICAL STUDY

(1) Assumptions

A part of an arch cut off by two adjacent points will be called an element of arch, and the displacements of the arches are described by the position of the centroids of their cross sections. The fundamental equations and extended formulations are derived on the following assumptions and idealizations.

1) The cross section of arched rib is bisymmetrical and uniform within each element. The arch of nonuniform cross section may be analyzed after dividing it into uniform elements of adequate length. 2) The warping rigidity and the effect of polar moment of inertia of arched ribs are disregarded. 3) Centroidal axes of the arches are inextensible.

* Graduate Student of Doctor Course, Graduate School of Eng., Osaka Univ.
** Dr. Eng., Chief Research Engineer of Structural Engineering Laboratory, Kobe Steel, Ltd., Formerly Associate Professor of Civil Eng., Osaka Univ.

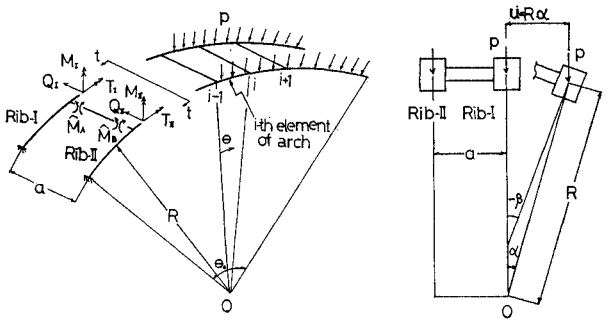

(a) Double arches with transverse bars (b) Section t-t

Fig. 1 General view

4) Uniformly distributed radial forces, p, are loaded at the centroids of cross sections of arched ribs. 5) The forces do not change their directions during the process of buckling (see Fig. 1 (b)). 6) The connection between arched ribs and transverse bars are completely rigid. 7) Influence of shear forces of transverse bars upon the buckling load is disregarded.

(2) Fundamental Equation and its Solution

Through consideration of an equilibrium of stress resultants and external forces acting on the i-th element of arched rib, following simultaneous differential equations with respect to the lateral deflection, α, and the torsional angle of cross section, β, can be derived (see Ref. 1) Eq. (30)).

That is,

$$\left.\begin{aligned}&\alpha''''+(\lambda_i-m_i)\alpha''-(1+m_i)\beta''=0\\&(1+m_i)\alpha''+m_i\beta''-\beta=0,\end{aligned}\right\}\quad\cdots(1)$$

where $\lambda_i=pR^3/EJ_i$, $m_i=GI_i/EJ_i$ and a prime superscript denotes one differentiation with respect to angular coordinate, θ. The symbols EJ_i and GI_i are flexural rigidity about out-of-plane bending and torsional rigidity of the i-th element, respectively. General solutions of these governing equations take different forms in compliance with the sign of $1-\lambda_i/m_i$ and are given as follows:

for $1-\lambda_i/m_i<0$,

$$\left.\begin{aligned}\alpha=&-\frac{m_ik_{1i}^2-1}{(1+m_i)k_{1i}^2}(C_1\cosh k_{1i}\theta+C_2\sin k_{1i}\theta)\\&-\frac{m_ik_{2i}^2+1}{(1+m_i)k_{2i}^2}(C_3\cos k_{2i}\theta+C_4\sin k_{2i}\theta)\\&+C_5\theta+C_6\\\beta=&C_1\cosh k_{1i}\theta+C_2\sinh k_{1i}\theta+C_3\cos k_{2i}\theta\\&+C_4\sin k_{2i}\theta,\end{aligned}\right\}\quad\cdots(2)$$

in which

$$\left.\begin{aligned}k_{1i}=&\sqrt{\frac{-\left(\frac{\lambda}{\mu_i}+2\right)+\sqrt{\left(\frac{\lambda}{\mu_i}+2\right)^2-4\left(1-\frac{\lambda}{\nu_im}\right)}}{2}}\\k_{2i}=&\sqrt{\frac{\left(\frac{\lambda}{\mu_i}+2\right)+\sqrt{\left(\frac{\lambda}{\mu_i}+2\right)^2-4\left(1-\frac{\lambda}{\nu_im}\right)}}{2}}\end{aligned}\right\}\quad\cdots(3)$$

$$\lambda=\frac{pR^3}{EJ_0},\quad m=\frac{GI_0}{EJ_0},\quad \mu_i=\frac{EJ_i}{EJ_0}$$

and $$\nu_i=\frac{GI_i}{GI_0}.\quad\cdots(4)$$

(The solution for $1-\lambda_i/m_i>0$ can be obtained similarly, and omitted here.)

The symbols EJ_0 and GI_0 denote the flexural rigidity and torsional rigidity of arched rib at the arch crown, respectively. Out-of-plane bending moment, M, torsional moment, T, and shear force directed outwards the arch plane, Q, are expressed in terms of displacements as follows:

$$\left.\begin{aligned}M=&\frac{EJ_i}{R}(\alpha''-\beta),\quad T=\frac{GI_i}{R}(\alpha'+\beta')\\Q=&-\frac{EJ_i}{R^2}(\alpha'''-\beta')+\frac{GI_i}{R^2}(\alpha'+\beta').\end{aligned}\right\}\quad\cdots(5)$$

Substituting Eq. (2) into Eq. (5), and denoting the non-dimensional quantities, TR/GI_0, MR/GI_0 and QR^2/GI_0 by the symbols $\overline{T}$, $\overline{M}$ and $\overline{Q}$, respectively, Eq. (5) yields for $1-\lambda_i/m_i<0$,

$$\left.\begin{aligned}\overline{M}=&-\nu_i\frac{k_{1i}^2+1}{m_i+1}(C_1\cosh k_{1i}\theta+C_2\sinh k_{1i}\theta)\\&+\nu_i\frac{k_{2i}^2-1}{m_i+1}(C_3\cos k_{2i}\theta+C_4\sin k_{2i}\theta)\\\overline{T}=&\nu_i\frac{1+k_{1i}^2}{k_{1i}(1+m_i)}(C_1\sinh k_{1i}\theta+C_2\cosh k_{1i}\theta)\\&+\nu_i\frac{1-k_{2i}^2}{k_{2i}(1+m_i)}(C_3\,k_{2i}\theta-C_4\sinh\cosh k_{2i}\theta)\\&+\nu_iC_5\\\overline{Q}=&\nu_i\frac{(k_{1i}^2+1)^2}{k_{1i}(1+m_i)}(C_1\sinh k_{1i}\theta+C_2\cosh k_{1i}\theta)\\&+\nu_i\frac{(k_{2i}^2-1)^2}{k_{2i}(1+m_i)}(C_3\sin k_{2i}\theta-C_4\cos k_{2i}\theta)\\&+\nu_iC_5.\end{aligned}\right\}\quad\cdots(6)$$

(3) Derivation of Field Matrix

First, let us take α, α', β, $\overline{T}$, $\overline{M}$ and $\overline{Q}$ as the elements of state vector $\boldsymbol{Z}_i$. That is,

$$\boldsymbol{Z}_i=\{\alpha,\ \alpha',\beta,\ \overline{T},\ \overline{M},\ \overline{Q}\}_i\quad\cdots(7)$$

in column vector form. This state vector, $\boldsymbol{Z}_i$, can be related to the arbitrary constant, $\boldsymbol{C}_i$, in matrix form as follows:

$$\tilde{\boldsymbol{Z}}_i(\theta)=\boldsymbol{B}_i(\theta)\cdot\boldsymbol{C}.\quad\cdots(8)$$

Hence, the state vector of intersection points $i-1$ and i will be expressed as

$$\tilde{\boldsymbol{Z}}_{i-1}=\boldsymbol{B}_i(0)\cdot\boldsymbol{C}\quad\cdots(9)$$

and

$$\tilde{\boldsymbol{Z}}_i=\boldsymbol{B}_i(\theta_i)\cdot\boldsymbol{C}.\quad\cdots(10)$$

Solving Eq. (9) with respect to $\boldsymbol{C}$ and substituting

it into Eq. (10) yields

$$\tilde{\boldsymbol{Z}}_i^L=\tilde{\boldsymbol{F}}_i\cdot\tilde{\boldsymbol{Z}}_{i-1}{}^R \quad \cdots\cdots(11)$$

in which

$$\tilde{\boldsymbol{F}}_i=\boldsymbol{B}_i(\theta_i)\cdot\boldsymbol{B}_i^{-1}(0), \quad \cdots\cdots(12)$$

and the subscripts L and R denote the left-hand side and the right-hand side of each intersection point, respectively. For the convenience of explanation, let us express the field matrix in simple notations of square submatrices of order 3 as follows :

$$\tilde{\boldsymbol{F}}_i=\left[\begin{array}{c|c}\boldsymbol{S} & \boldsymbol{U}\\ \hline \boldsymbol{V} & \boldsymbol{W}\end{array}\right]. \quad \cdots\cdots(13)$$

In the above discussion, attention is paid to one of the double ribs. Then, in order to transfer the quantities of both rib-I and rib-II simultaneously, let us take the column vector,

$$\boldsymbol{Z}_i=\{\alpha_{\mathrm{I}},\ \alpha_{\mathrm{I}}',\ \beta_{\mathrm{I}},\ \alpha_{\mathrm{II}},\ \alpha_{\mathrm{II}}',\ \beta_{\mathrm{II}},\ \overline{T}_{\mathrm{II}},\ \overline{M}_{\mathrm{II}},\ \overline{Q}_{\mathrm{II}},\ \overline{T}_{\mathrm{I}},\ \overline{M}_{\mathrm{I}},\ \overline{Q}_{\mathrm{I}}\}_i \quad \cdots\cdots(14)$$

as the state vector of the intersection point i, where the symbols with the subscripts I and II indicate the quantities with respect to rib-I and rib-II, respectively. The overall relation between the state vector of the intersection point i and that of the intersection point $i-1$ will be given by

$$\boldsymbol{Z}_i^L=\boldsymbol{F}_i(\theta)\cdot\boldsymbol{Z}_{i-1}{}^R \quad \cdots\cdots(15)$$

where

$$\boldsymbol{F}_i(\theta)=\left[\begin{array}{c|c|c|c}\boldsymbol{S}_{\mathrm{I}} & \boldsymbol{0} & \boldsymbol{0} & \boldsymbol{U}_{\mathrm{I}}\\ \hline \boldsymbol{0} & \boldsymbol{S}_{\mathrm{II}} & \boldsymbol{U}_{\mathrm{II}} & \boldsymbol{0}\\ \hline \boldsymbol{0} & \boldsymbol{V}_{\mathrm{II}} & \boldsymbol{W}_{\mathrm{II}} & \boldsymbol{0}\\ \hline \boldsymbol{V}_{\mathrm{I}} & \boldsymbol{0} & \boldsymbol{0} & \boldsymbol{W}_{\mathrm{I}}\end{array}\right] \quad \cdots\cdots(16)$$

(4) Derivation of Point Matrix

First of all, let us imagine that the transverse bars are connected to the arched rib as one of the principal axes of transverse bar is always horizontal (see Fig. 2(c)) and only the flexural rigidity with respect to the horizontal principal axis is considered (let us call Type-V). Considering an arbitrary transverse bar cut off like what illustrated in Fig. 2, the relation between the flexural moments of transverse bar, $\hat{M}_A$ and $\hat{M}_B$, and the deformations of arched rib, α' and β, is shown as

$$\left[\begin{array}{c}\hat{M}_A\\ \hat{M}_B\end{array}\right]=\left[\begin{array}{cc}\dfrac{4E\hat{J}_i}{a} & \dfrac{2E\hat{J}_i}{a}\\ -\dfrac{2E\hat{J}_i}{a} & -\dfrac{4E\hat{J}_i}{a}\end{array}\right]\cdot\left[\begin{array}{cccc}\sin\bar{\theta}_i & -\cos\bar{\theta}_i & 0 & 0\\ 0 & 0 & \sin\bar{\theta}_i & -\cos\bar{\theta}_i\end{array}\right]\cdot\left[\begin{array}{c}\beta_{\mathrm{I}}\\ \alpha_{\mathrm{I}}'\\ \beta_{\mathrm{II}}\\ \alpha_{\mathrm{II}}'\end{array}\right] \quad \cdots\cdots(17)$$

in which the symbols a, $E\hat{J}_i$ and $\bar{\theta}_i$ denote the distance between rib-I and rib-II, flexural rigidity of i-th transverse bar and the angle between a horizontal line and the radius $A-0$, respectively. The equilibrium equations around the point A are

$$\left.\begin{array}{l}M_{\mathrm{I}}{}^R=M_{\mathrm{I}}{}^L-\hat{M}_A\cos\bar{\theta}_i,\\ T_{\mathrm{I}}{}^R=T_{\mathrm{I}}{}^L+\hat{M}_A\sin\bar{\theta}_i\end{array}\right\} \quad \cdots\cdots(18)$$

and $Q_{\mathrm{I}}{}^R=Q_{\mathrm{I}}{}^L$.

As for the rib-II, in the same manner, the equilibrium equations are :

$$\left.\begin{array}{l}M_{\mathrm{II}}{}^R=M_{\mathrm{II}}{}^L+\hat{M}_B\cos\bar{\theta}_i,\\ T_{\mathrm{II}}{}^R=T_{\mathrm{II}}{}^L-\hat{M}_B\sin\bar{\theta}_i\end{array}\right\} \quad \cdots\cdots(19)$$

and $Q_{\mathrm{II}}{}^R=Q_{\mathrm{II}}{}^L$.

The deformations α, α' and β will hold continuity from the left-hand side to the right-hand side of the intersection point i.Then, substituting Eq. (17) into Eqs. (18) and (19), and introducing non-dimensional quantity, $r_i=E\hat{J}_i/GI_0\cdot R/a$, yield

$$\boldsymbol{Z}_i^R=\boldsymbol{P}_i(\bar{\theta}_i)\cdot\boldsymbol{Z}_i^L, \quad \cdots\cdots(20)$$

where

$$\boldsymbol{P}_i(\bar{\theta}_i)=\left[\begin{array}{cccccc}1 & & & & & \\ & 1 & & \boldsymbol{0} & & \\ & & 1 & & & \\ & \boldsymbol{0} & & 1 & & \\ & & & & 1 & \\ \hline 0 & \boldsymbol{X} & 0 & \boldsymbol{Y} & 1 & \\ 0 & & 0 & & 1 & \boldsymbol{0}\\ 0 & 0 & 0 & 0 & 0 & 1\\ 0 & \boldsymbol{Y} & 0 & \boldsymbol{X} & \boldsymbol{0} & 1\\ 0 & 0 & 0 & 0 & 0 & 1\end{array}\right] \quad \cdots\cdots(21)$$

$$\boldsymbol{X}=\left[\begin{array}{cc}-2r_i\sin\bar{\theta}_i\cos\bar{\theta}_i & 2r_i\sin^2\bar{\theta}_i\\ 2r_i\cos^2\bar{\theta}_i & -2r_i\sin\bar{\theta}_i\cos\bar{\theta}_i\end{array}\right]$$

$$\boldsymbol{Y}=\left[\begin{array}{cc}-4r_i\sin\bar{\theta}_i\cos\bar{\theta}_i & 4r_i\sin^2\bar{\theta}_i\\ 4r_i\cos^2\bar{\theta}_i & -4r_i\sin\bar{\theta}_i\cos\bar{\theta}_i\end{array}\right] \quad \cdots\cdots(22)$$

By the way, when the transverse bar is connected to the arched rib ars one of the principal axes of transverse bar is perpendicular to the longitudinal axis of arched rib (let us call Type-P), the submatrices, X and Y, of Eq. (21) will be obtained

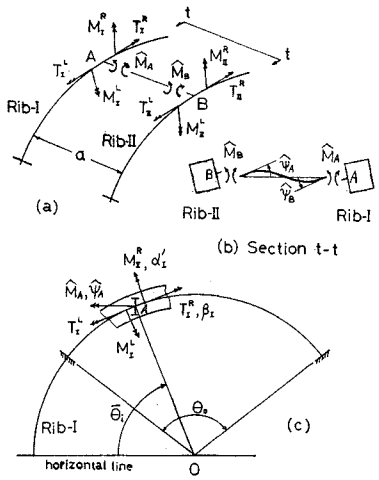

Fig. 2 Equilibrium around an i-th transverse bar (Type-V)

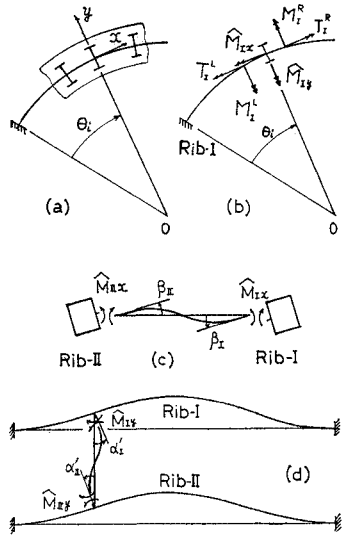

Fig. 3 Transverse bar of Type-P

as follows after a similar deduction shown above (see Fig. 3). In this case, both the flexural rigidity with respect to x-axis, $E\hat{J}_x$, and that with respect to y-axis, $E\hat{J}_y$, are considered. That is,

$$\boldsymbol{X}=\begin{bmatrix}0 & 2\kappa r_y\\ 2r_y & 0\end{bmatrix}_i \text{ and } \boldsymbol{Y}=\begin{bmatrix}0 & 4\kappa r_y\\ 4r_y & 0\end{bmatrix}_i, \quad \cdots(23)$$

where

$$(r_y)_i=\frac{(E\hat{J}_y)_i}{GI_0}\cdot\frac{R}{a} \text{ and } \kappa_i=\left(\frac{\hat{J}_x}{\hat{J}_y}\right)_i \cdots(24)$$

(5) General Procedure of Transfer Matrix

Substituting Eq. (15) into Eq. (20) yields

$$\boldsymbol{Z}_i{}^R=\boldsymbol{P}_i\cdot\boldsymbol{F}_i\cdot\boldsymbol{Z}_{i-1}{}^R \quad \cdots(25)$$

Repeating this procedure from point to point, the state vector of the right-hand end of the arch can be related to that of the left-hand end of the arch. That is,

$$\boldsymbol{Z}_n{}^L=\boldsymbol{F}_n\cdot\boldsymbol{P}_{n-1}\cdots\boldsymbol{F}_i\cdot\boldsymbol{P}_{i-1}\cdot\boldsymbol{F}_{i-1}\cdots \boldsymbol{P}_1\cdot\boldsymbol{F}_1\cdot\boldsymbol{Z}_0{}^R=\boldsymbol{T}\cdot\boldsymbol{Z}_0{}^R \quad \cdots(26)$$

The matrix $\boldsymbol{T}$ takes usually a square matrix form of order 12 and each element contains the buckling coefficient, λ, as an unknown variable.

(6) Boundary Conditions and Coefficient Determinant

Two sorts of boundary conditions are considered. First, when the both arch ends are rigidly fixed, the boundary conditions are

$$\left.\begin{array}{l}\text{at } \theta=0,\ \alpha_{\mathrm{I}}=\alpha_{\mathrm{I}}{}'=\beta_{\mathrm{I}}=\alpha_{\mathrm{II}}=\alpha_{\mathrm{II}}{}'=\beta_{\mathrm{II}}=0\\ \text{and at } \theta=\theta_0,\ \alpha_{\mathrm{I}}=\alpha_{\mathrm{I}}{}'=\beta_{\mathrm{I}}=\alpha_{\mathrm{II}}=\alpha_{\mathrm{II}}{}'=\beta_{\mathrm{II}}=0.\end{array}\right\} \quad \cdots(27)$$

Substituting Eq. (27) into Eq. (26) yields six homogeneous equations. For non-trivial solution of these equations, the determinant of the coefficients must be zero. Hence, the buckling condition is

$$\boldsymbol{D}(\lambda)=\begin{vmatrix} t_{1,7} & t_{1,8} & t_{1,9} & t_{1,10} & t_{1,11} & t_{1,12}\\ t_{2,7} & t_{2,8} & t_{2,9} & t_{2,10} & t_{2,11} & t_{2,12}\\ t_{3,7} & t_{3,8} & t_{3,9} & t_{3,10} & t_{3,11} & t_{3,12}\\ t_{4,7} & t_{4,8} & t_{4,9} & t_{4,10} & t_{4,11} & t_{4,12}\\ t_{5,7} & t_{5,8} & t_{5,9} & t_{5,10} & t_{5,11} & t_{5,12}\\ t_{6,7} & t_{6,8} & t_{6,9} & t_{6,10} & t_{6,11} & t_{6,12}\end{vmatrix}=0 \cdots(28)$$

The lowest positive value satisfying this condition is the critical value of λ. Next, when the both arch ends are hinged, the boundary conditions are

$$\left.\begin{array}{l}\text{at } \theta=0,\ \alpha_{\mathrm{I}}=\beta_{\mathrm{I}}=\alpha_{\mathrm{II}}=\beta_{\mathrm{II}}=0,\ \bar{M}_{\mathrm{I}}=\bar{M}_{\mathrm{II}}=0\\ \text{and at } \theta=\theta_0,\ \alpha_{\mathrm{I}}=\beta_{\mathrm{I}}=\alpha_{\mathrm{II}}=\beta_{\mathrm{II}}=0,\ \bar{M}_{\mathrm{I}}=\bar{M}_{\mathrm{II}}=0\end{array}\right\} \quad \cdots(29)$$

Substituting Eq. (29) into Eq. (26), in the same manner shown above, yields the buckling condition of this case.

(7) Numerical Procedure and Some Problems

The solution of Eq. (28) is obtained by means of trial and error method as a value of λ_j which satisfies the relation $D(\lambda_j)\cdot D(\lambda_j+\Delta\lambda)\leq 0$, where $\Delta\lambda$ is the buckling-coefficient increment. As for the magnitude of $\Delta\lambda$, the larger the better for shortening the computation time, but a large increment involves a risk of failing to catch the positive-minimum solution. Since even a small increment, $\Delta\lambda$, will produce a large and sharp fluctuation of $D(\lambda)$, particularly in the region near the solution, special attention must be paid in determining the magnitude of $\Delta\lambda$. Further, with respect to a certain combination of the values, m and λ, the value of $D(\lambda)$ may fail to vanish at where it must be zero, owing to the accumulated errors and lack of significant digits. This deficiency was conquered by tracing the value of $D(\lambda)$ and the missing solutions were presumed from the shape of the curve of $D(\lambda)$.

Table 1 Connecting direction of transverse bar

Type-V	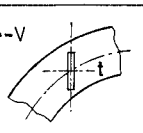	One of principal axes is vertical and only $\hat{J}_t$ is considered. $\gamma_t=\frac{E\hat{J}_t}{GI_0}\frac{R}{a}$
Type-P	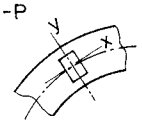	One of principal axes is perpendicular to the centroidal axis of arched rib, and both $\hat{J}_x$ and $\hat{J}_y$ are considered. $\gamma_y=\frac{E\hat{J}_y}{GI_0}\frac{R}{a}$, $\kappa=\frac{\hat{J}_x}{\hat{J}_y}$ and $\gamma_x=\frac{E\hat{J}_x}{GI}\frac{R}{a}$
Type-L	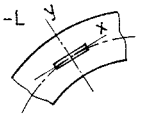	$\hat{J}_x=0$ in Type-P; $\gamma_y=\frac{E\hat{J}_y}{GI_0}\frac{R}{a}$, $\kappa=\gamma_x=0$

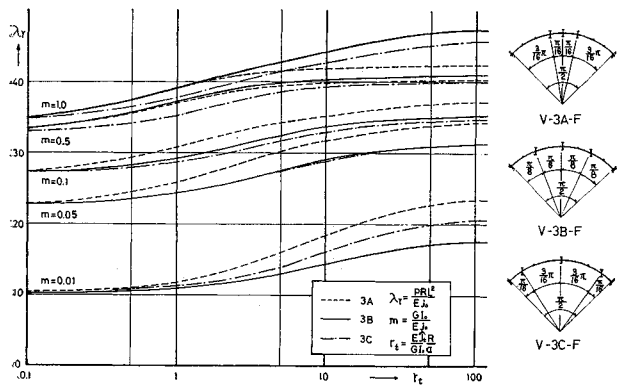

Fig. 4 Buckling coefficient for three transverse bars (Fixed end)

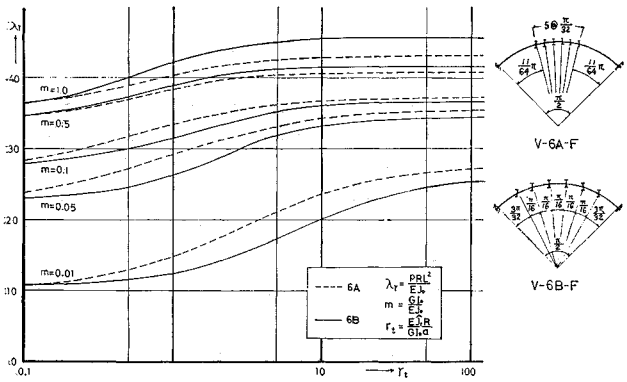

Fig. 5 Buckling coefficient for six transverse bars (Fixed end)

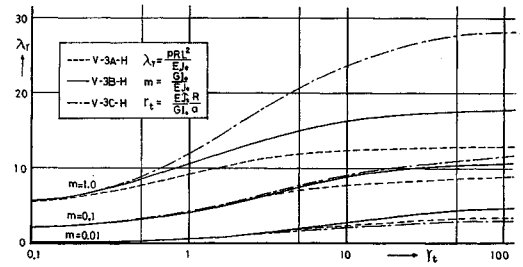

Fig. 6 Buckling coefficient for three transverse bars (Hinged end)

(8) Results and Consideration

Several numerical examples are shown below. Since the symmetrical buckling of first mode will give the smallest critical value, all computations were performed about it. In these numerical examples, the cross sections of the main ribs are constant through the arch span and all the transverse bars of each intersection point have same cross section, and further central angle, θ_0, of the arch is right angle for all cases. Accordingly, $\nu_i=\mu_i=1$

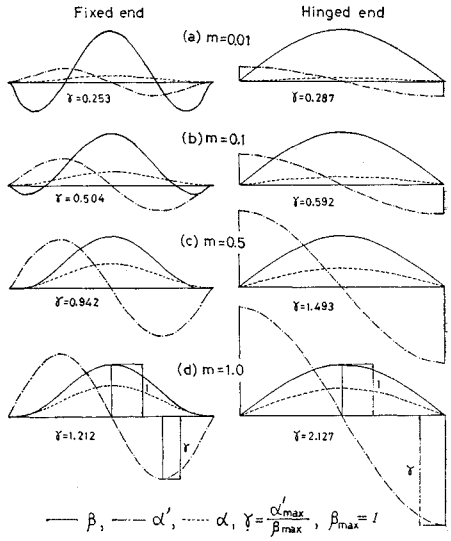

Fig. 7 Shape of buckling mode of single arch

and r_i $(i=1, 2,\cdots)=r_t$. Computation cases are expressed as V-3 A-H or P-6 B-F, etc.. The meaning of the first letter is explained in Table 1. Type-P and Type-L are imagined to repesent the transverse bars of actual arch bridges which mainly resist to torsion of the arched ribsand lateral bracings of actual arch bridges which resist only to lateral bending of the arched ribs, respecti vely. The second letters mean the number and the manner of arrangement of the transverse bars. The last letter means the end condition of arches, fixed or hinged. In the figures, the buckling coefficient, λ_r, is defined as pRL^2/EJ_0, where L is arc-length of the arch. The magnitude of m will be, in general,

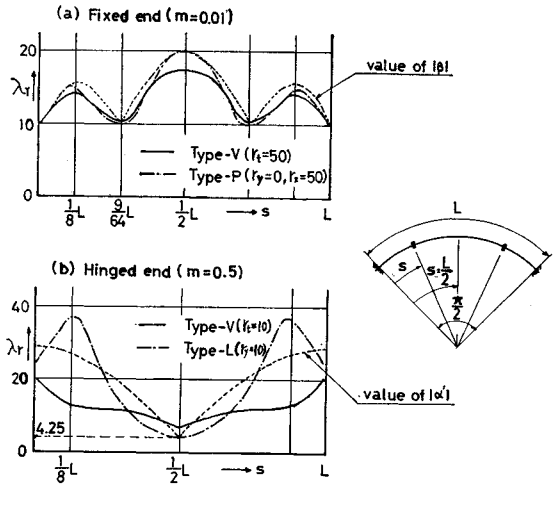

Fig. 8 Influence of position of transverse bars

from 0.1 to 1.0 for a closed cross section and from 0.1 to 10^{-3} for a open cross section. In numerical computation, digital computer (NEAC 2200-500) of the computer center of Osaka Univ. was used. Several discussions and characteristics about the influences of the bracing bars on the buckling strength are given below.

1) Flexural rigidities r_t and r_x (see Figs. 4 and 5)

From the nature of things, with the increase of r_t, the buckling coefficient, λ_r, becomes large. For $r_t \to 0$, the ordinates of the curves, as it should, approach the values of the buckling coefficients of single arch. The influence of r_t is remarkable for the small value of m. For example, the buckling coefficeint of the case V-6 B-F ($m=0.01$) attains 2.5 times of that of single arch. The limiting value of λ_r are given at about $r_t=1/m$ for all cases. There is little difference between the influence of r_x and that of r_t. The λ_r versus r_x curves of the case P-3 B-F ($r_y=0$) practically coincide with those of case V-3 B-F, and so are not shown in the figure.

2) Number of transverse bars

The buckling strength becomes large with the increase of the number of transverse bars, but the magnitude of increase is not so considerable except the case of $m=0.01$.

3) Arrangement of transverse bars

In Fig. 4, the influence of the arrangement is not so remarkable except the case of $m=0.01$. In the case of $m=0.01$, relative magnitude of the ordinates of the curves is case-3 A>case-3 C>case-3 B. This result implies that the influence of the arrangement have close relation to the shape of buckling mode shown in Fig. 7 (note the magnitude of γ which is uniquely determined against a unique value of m). In order to confirm this idea, the buckling coefficient of arches braced with two transverse bars in various positions were computed and plotted at the each position of the transverse bars. The curve showing influence of position of the transverse bars upon λ_r and the curve showing the value of $|\beta|$ (absolute value of the torsional angle, β) are similar in shape (Fig. 8(a)). In the range of the large value of m, this influence does not appear, because arched ribs of closed cross secton will not show so large deformation in torsion. As for the arches of hinged end (Fig. 6), the influence of the arrangement occurs in the range of large value of m (at the same time, large value of γ) and is relative to the magnitude of α' of that location (see Fig. 8(b)). Furthermore, Fig. 8 (b) implies that the flexural rigidity, r_y, near the arch end improves the buckling strength of hinged-end arches remarkably.

4) Flexural rigidity r_y (see Fig. 9)

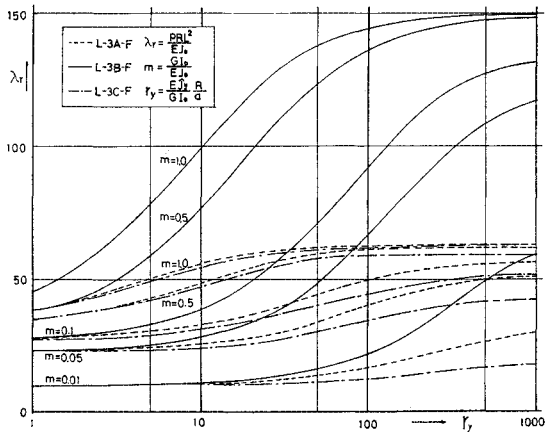

Fig. 9 Buckling coefficient of Type-L (Fixed end)

The influences of r_y are illustrated in Fig. 9 as the form of λ_r versus r_y curves. Through above discussion it is easy to interprete these results. Namely, since r_y is directly relative to α', the significant differences of location appear in the range of large value of m (large value of γ). The ordinates of the case-3 B whose side-transverse bars are located at $L/4$ points, where the magnitude of α' is maximum (see Fig. 7(d)), are quite larger than those of other two cases. The limiting ordinates are attained at about $r_y=100/m$ for all cases of three transverse bars and at about $r_y=10/m$ for all cases of six transverse bars.

5) End condition of arched ribs

The buckling strength of hinged-end arch reduces remarkably. This fact implies that even a slight loose of the fixed end may lead the arch bridges to collapse. The practical significance of this observation is obvious, since in actual arch bridges, completely rigid supports are difficult, if not possible, to realize.

3. MODEL TEST

Several model tests were conducted and one of them are shown below.

(1) Model Arch

Tested model arch is shown in Fig. 10. Both the main ribs and the transverse bars are made of brass and the model arches were assembled by means of solder connection.

(2) Apparatus and Procedure of Experiment

Particular attention was paid in fitting up the model arch not to produce initial lack of fit. The end of the ribs were built-in to an steel plate which is supported as to rotate freely about the

axis perpendicular to the arch plane. In order to prevent slipping and to give full play to an arch action, the ends of the arches were carefully fixed against horizontal displacements. Since it is difficult to realize a distributed radial load, group of vertical concentrated loads was applied in place of it. The loading devices are shown in Photo 1. The piano wire were used as to follow the displacement outward the arch plane without restraint, but the excentricity of loading was inevitable because of the cross-sectional shape of model arch. The loading rod was pulled downward by a hydraulic jack. Model arch was loaded gardually and carefully not to produce disturbance.

	Theoretical values			Experimental values		$\frac{\bar{P}_E}{P_T}\times 100$ (%)
	λr	P_{cr}(kg/cm)	$P_T=2P_{cr}L$(kg)	P_E(kg)	$\bar{P}_E=P_E\left(\frac{\theta_0}{\sin\theta_0}\right)^{1)}$(kg)	
Model arch	40.0	7.9	1754	1400	1555	88.6
Single arch	32.25	6.29	1398	—	—	—

Table 2 Theoretical and experimental buckling load

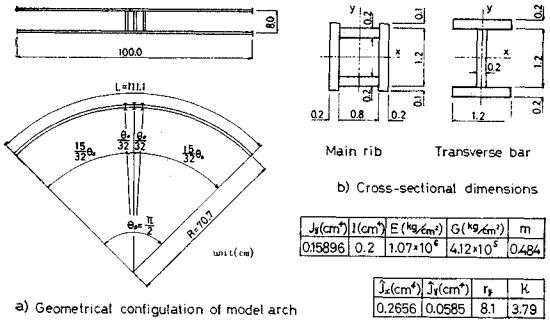

J_y(cm⁴)	I(cm⁴)	E(kg/cm²)	G(kg/cm²)	m
0.15896	0.2	1.07×10^6	4.12×10^5	0.484

J_x(cm⁴)	J_y(cm⁴)	r_g	K
0.2656	0.0585	8.1	3.79

Fig. 10 Model arch

Photo 1 Loading devices

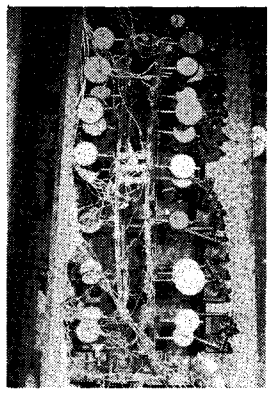

Photo 2 Critical equilibrium state at $P=1.35$ ton

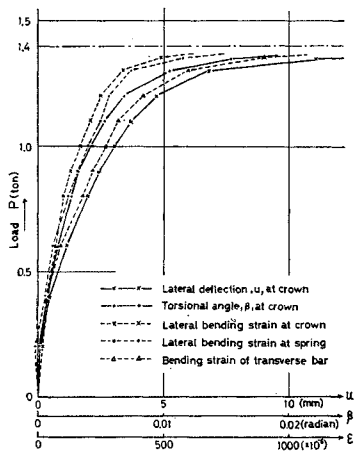

Fig. 11 Load vs. deformation curves

(3) Results and Consideration

The ultimate load was estimated as $P=1.40$ t from the asymptote of the load-deformation curves. The model arch in critical equilibrium state at $P=1.35$ t is shown in Photo 2. Test results are illustrated in Fig. 11. These curves show the effects of initial imperfection in lower range of loading, but to avoid them was, actually, difficult. Both the buckling load obtained from the theoretical analysis and model test are shown in Table 2. The experimental value shows about 90%-coincidence with the theoretical one.

4. CONCLUSIONS

The following conclusions will be drawn within the scope of the given assumptions and idealizations :

1) Transfer matrix method was employed effectively in obtaining the eigenvalue of the differential equation governing the buckling of complicated structures which consist of main systems and branch systems.

2) Results of numerical computation about several arches are illustrated as the curves of buckling coefficient versus flexural rigidity of the transverse bars.

3) The arrangement of the transverse bars are in close relation to the shape of buckling mode of corresponding single arch. To arrange the transverse bars of large flexural rigidity at the location where corresponding large deformations of the arched ribs occurs is effective from the view point of lateral stability. That may be, in other words, to increase the total strain energy stored in the transverse bars during the buckling deformation.

4) In order to interprete the relation between the cross-sectional quantities of the arched rib and the effects of transverse bars, the ratio, r, of the maximum value of the torsional angle, β_{max}, to that of lateral deflection angle, α_{max}' are quite

important.

5) The location of the transverse bars are more important than the number of them.

6) In order to increase the buckling strength of the arch bridges as treated in this paper, to constrain the out-of-plane flexure of arched rib is much more effective than to constrain the torsional deformation of arched rib. In other words, lateral bracings which resist to the out-of-plane flexure may be more effective than the transverse bars of Vierendeel type.

7) A slight loose of the fixed end about the out-of-plane rotation may lose the buckling strength of the arch bridges practically.

ACKNOWLEDGMENTS

The authors are greatly indebted to Professor Dr. S. Komatsu for his important advice and encouragement. Furthermore, acknowledgment due to Mr. M. Taga for his co-operation in the experiments and to Mr. Y. Iwahana for part of numerical computations. This study was performed under Financial Support of Ministry of Education.

REFERENCES

1) Namita, Y. : Die Theorie II. Ordnung von Krummen Stäben und ihre Anwendung auf das Kipp-Problem des Bogenträgers, Trans. of J.S.C.E., No. 155, 1968 (in German).
2) Kuranishi, S. : Torsional Buckling Strength of Solid Rib Arch Bridge, Trans. of J.S.C.E., No. 75, 1961 (in Japanese).
3) Östlund, L. : Lateral Stability of Bridge Arches braced with Transverse Bars, Trans. of the Royal Institute of Technology, Stockholm, Sweden, No. 84, 1954.
4) Wästlund, G. : Stability Problems of Compressed Steel Members and Arch Bridges, Proc. of A.S.C.E., Vol. 86, St 6, June, 1960.
5) Kuranishi, S. : Analysis of Arch Bridge under certain Lateral Forces, Trans. of J.S.C.E., No. 73, 1961 (in Japanese).
6) Fukasawa, Y. : Buckling of Circular Arches by Lateral Flexure and Torsion under Axial Thrust, Trans. of J.S.C.E., No. 96, 1963 (in Japanese).
7) Pestel, E.C. and Leckie, F.A. : Matrix Method in Elastomechanics, McGraw-Hill, 1963.
8) Okumura, A. : On a Method of Analysis for Vibration and Stability Problems of Linear Mechanical Systems or Structures, Memories of the School of Science and Engineering, Waseda Univ., No. 21, 1957.
9) Shibata, M. : An Analysis for Vibration of Structures by Transfer Matrix Method, Journal of J.S.S.C., Vol. 3, No. 24, 1967 and Vol. 4, No. 27, 1968 (in Japanese).
10) Margurre, K. : Vibration and Stability Problems of Beams Treated by Matrices, Journal of Mathe. and Physics, Vol. 35-1, 1956.

(Recived Nov. 14, 1970)